The evolution of classical doubles: clues from complete samples

Katherine M. Blundell
Oxford University Astrophysics, Keble Road, Oxford, OX1 3RH, UK
E-mail: kmb@astro.ox.ac.uk

Steve Rawlings
Oxford University Astrophysics, Keble Road, Oxford, OX1 3RH, UK

Chris J. Willott
Instituto de Astrofisica de Canarias, 38200 La Laguna, Tenerife, Spain

We describe the inter-dependence of four properties of classical double radio sources — spectral index, linear size, luminosity and redshift — from an extensive study based on spectroscopically-identified complete samples. We use these relationships to discuss aspects of strategies for searching for radio galaxies at extreme redshifts, in the context of possible capabilities of the new generation of proposed radio telescopes.

1 Introduction

In the beginning, nearly [1], was the 3C sample of radio sources. This was a very good sample of radio sources, except that it suffered from a problem which afflicts each and every single flux-limited sample: the luminosity–redshift (P–z) degeneracy. This tight correlation between luminosity and redshift is illustrated schematically in Fig. 1, for the case of the 3C sample.

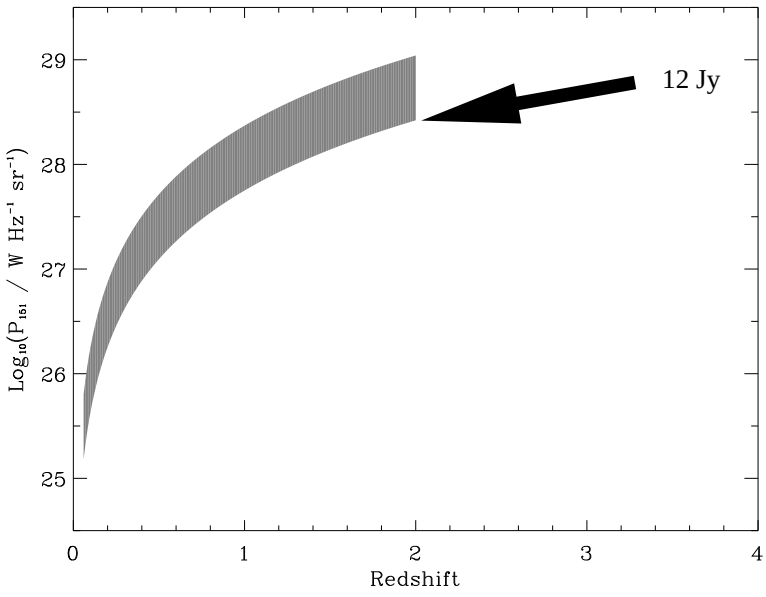

Figure 1: The shaded area represents the coverage of the P–z plane by the 3C sample. It demonstrates the tight correlation between luminosity and redshift inherent in any single flux-limited sample. The lower boundary of the shaded region corresponds to a flux-limit of 12 Jy at 151 MHz in a Universe with $\Omega_{\rm M} = 1$ and $\Omega_\Lambda = 0$, and assuming the radio sources have a low-frequency spectral index $\alpha = 1$, with $S_\nu \propto \nu^{-\alpha}$, where S_ν is the flux density at frequency ν.

In order to decouple radio source properties which primarily depend on luminosity from those which depend on redshift, it is necessary to increase substantially coverage of the P–z plane over that

occupied by the 3C sample. We have done this by pursuing a programme of identifying faint complete samples of radio sources from 6C and 7C, selected at low frequencies similar to 3C [2]. By selecting samples of radio sources with significantly lower flux-limits than 3C we find more lower-luminosity objects than known before at high redshift, thus breaking the P–z degeneracy. A *combination* of complete samples makes this possible.

2 Linear-size evolution revisited

It has been known for many years that the linear sizes of classical double radio sources appear to become smaller with increasing redshift [3]. However, it has not been clear until recently that this is primarily a dependence of linear size on redshift rather than arising because of an anti-correlation of linear size and luminosity [4, 5].

In fact the observed linear size evolution is *an artifact of the survey process itself.* How strong this is found to be depends crucially on the *finding-frequency* of the samples used in the study. For example, when the finding-frequencies are quite different for the brighter and the fainter samples (e.g. 151 MHz with a 12 Jy flux-limit and 408 MHz with a 1 Jy flux-limit) as in the case of [6]) then a very strong evolution of linear size (D) with redshift is observed which may be parameterised as $D \propto (1+z)^{-3.5}$. When the finding-frequencies of the samples are the same, the linear size evolution is found to be substantially milder [5], and obeys the parameterisation $D \propto (1+z)^{-1.3}$. The mildness of the linear size evolution in this region of source parameter space is very similar to that found [10] for samples selected at 151 MHz brighter than 12 Jy and at 38 MHz brighter than 1.3 Jy.

The linear size a radio source has acquired when selected by a survey depends on both its underlying jet-power and the environmental profile into which it is expanding, and also on the length of time elapsed since the jets first began expanding, that is, on the *age of the radio source.*

3 What do hotspots do?

From the earliest [7, 8] to the most recent [9, 5] models of radio-source evolution, with reasonable assumptions about the environments into which radio sources expand, the luminosity of any individual radio source decreases as time, or age, increases. How dramatic this decrease is does depend on the assumed density gradient [9] but depends more dramatically on whether account is taken of the rôle which hotspots play in a radio-source [5]. Hotspots do not reside in classical double radio sources merely to facilitate measurement of angular sizes by the observer! Rather, they play a key rôle in the evolution of a radio source. We have modelled two aspects of this rôle [5].

First, the magnetic field of the hotspot causes significant radiative losses on synchrotron particles during their dwell-time in the hotspot, in the period of time before they are injected into the lobe. We were led to this by our observation that the radio sources in our complete samples seemed to strongly indicate that the more luminous a radio-source was, the steeper its *low-frequency spectrum* was (for example, when evaluated at rest-frame 151 MHz). This rest-frame frequency regime is less affected by synchrotron and inverse Compton losses than the GHz regime and thus informs us on the energy distribution of particles *as initially injected* into the lobe of a radio-source. Modelling a steeper spectrum in a more powerful source came naturally out of invoking stronger magnetic fields (hence stronger radiative losses) in sources with higher jet-powers. By equating the jet-thrust and the pressure in the compact hotspot, and invoking equipartition in the hotspot, we find that the magnetic energy density in the hotspot is proportional to the bulk kinetic power transported in the jet (see equation 11 in [5]).

Second, as a plasma element expands out of a compact hotspot into a lobe whose pressure is considerably lower (and continues to become lower as the radio source expands and gets older) it suffers enhanced adiabatic expansion losses compared to the expansion losses suffered by that element of plasma once it continues to dwell in the lobe. This is consistent with observations of classical doubles which invariably show highly compact hotspots — embedded towards the outermost edges of the smooth, low surface-brightness, extended emission which comprises the lobe — albeit with a bewildering menagerie of shapes and structures [17, 19, 18].

4 What governs the spectral indices at different frequencies?

In §3 we briefly described how a stronger hotspot magnetic field will result in a steeper energy distribution of particles being injected into the lobe, and hence a steeper measured spectral index at low-frequency in the rest-frame. This model consistently explains the P–α correlation we presented in [5].

Further losses cause a very different dependence of spectral index when this is evaluated in the GHz regime. In fact while we found the low-frequency regime spectral index to correlate with *luminosity*, we found the GHz-regime spectral index to correlate instead with *redshift.* This is illustrated in Fig. 2.

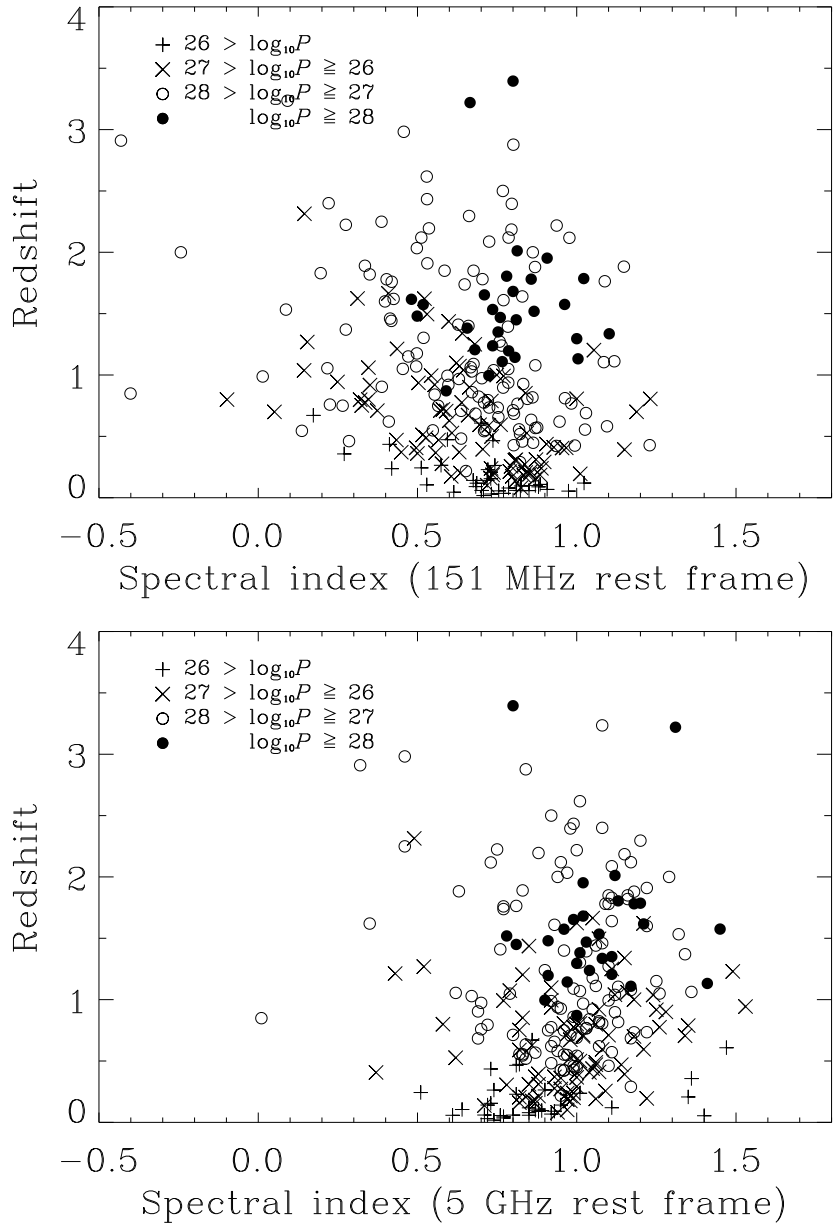

Figure 2: The upper panel plots the redshifts of the 3C, 6C and 7C objects versus their spectral indices evaluated at 151 MHz in their rest-frames. There is no evidence for any independent correlation between these two properties. The lower panel shows that when the spectral index is evaluated at 5 GHz in their rest-frames, this does significantly depend on redshift, indicating the increasing importance of inverse Compton losses in this frequency regime.

The low-frequency spectral indices of lobes are also found to increase with increasing linear size; this may be seen in Fig. 3.

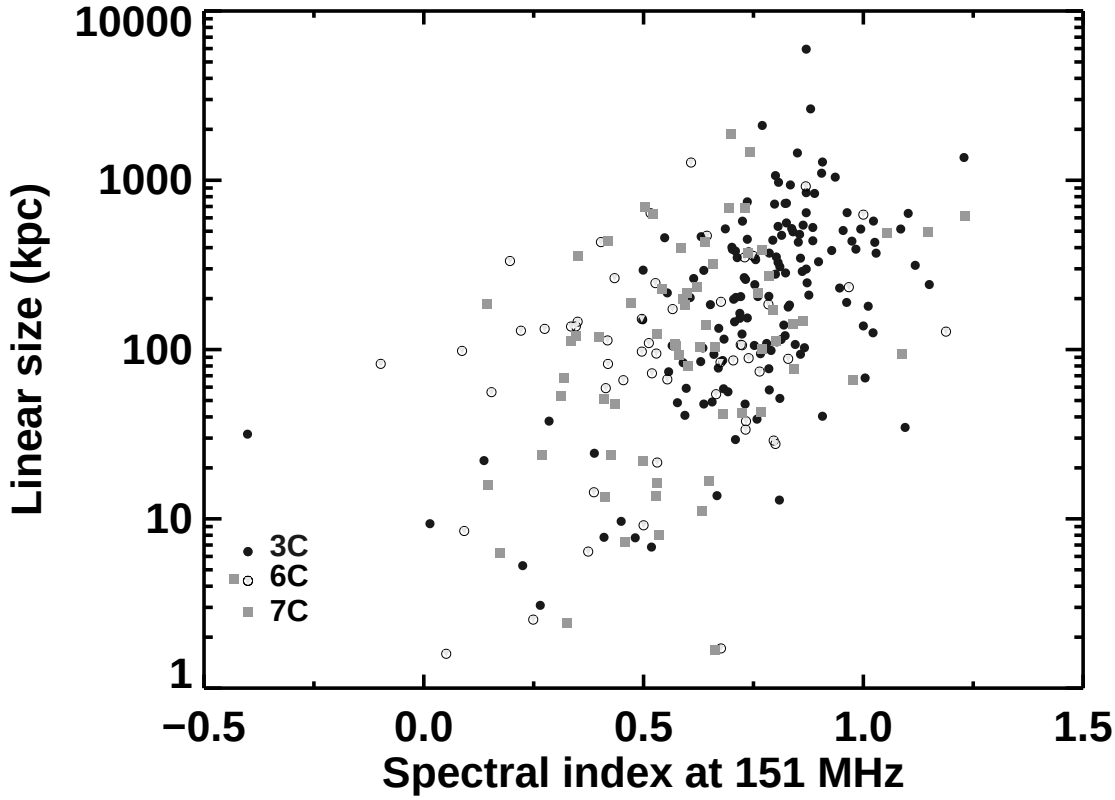

Figure 3: This plot shows the projected linear sizes of the 3C, 6C and 7C objects versus their spectral indices evaluated at 151 MHz in their rest-frames. These quantities are seen to be significantly correlated. Note that two competing effects are occuring: the P–α correlation, most manifest in the high-power sources and the D–α correlation, seen in the large linear-size, low-powered sources.

We interpret the D–α correlation as being due to the decrease in magnetic field as the lobes expand. For a fixed observing frequency, the Lorentz factors of particles contributing most of their emission at this frequency will be *higher* in a *lower* magnetic field since the frequency-dependence of synchrotron radiation from an electron with Lorentz factor γ in a magnetic field B is given by:

$$\gamma = \left(\frac{m_{\rm e}}{eB} 2\pi\nu\right)^{\frac{1}{2}}, \tag{1}$$

where $m_{\rm e}$ is the rest mass of an electron and e is the charge on an electron.

Thus as the radio-lobe expands and its magnetic field decreases particles with a higher Lorentz factor are required to radiate at the chosen observing frequency. Given the power-law exponent of typical energy distributions, the number of high Lorentz factor particles is smaller than the number of less energetic particles. Moreover, the adiabatic expansion of the lobes *per se*, while preserving the shape of the spectrum, will shift to lower frequencies any features in the spectrum such as a break frequency.

5 Where are the large, powerful radio sources?

Factoring in the rôle of the hotspot goes a long way to solving a problem nearly three decades old (see e.g. [8]), namely the dearth of large *and* powerful classical doubles. On the face of it this is puzzling: intuitively more powerful radio-sources should expand faster than those with lower jet-powers, so the laws of probability alone suggest it should be easy to find large, powerful sources. But they are not there: sources with $P > 10^{27}\,{\rm W\,Hz^{-1}\,sr^{-1}}$ and with $D > 1\,{\rm Mpc}$ are not found in existing surveys (see Fig. 4).

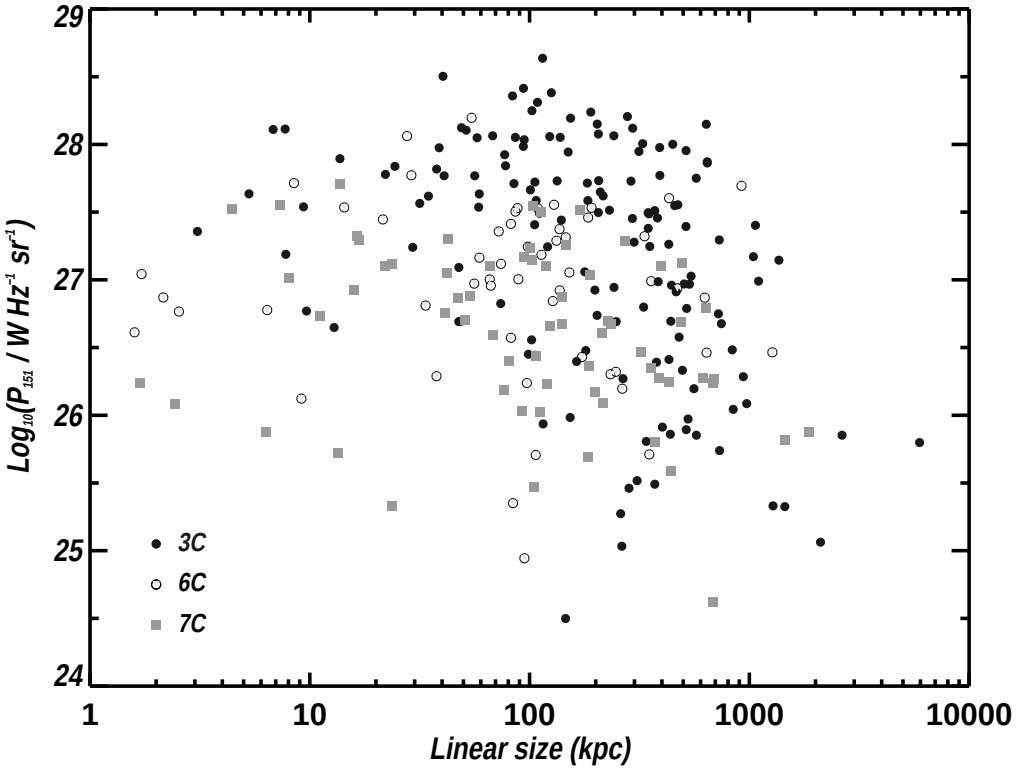

Figure 4: The 'P–D' plane for classical double radio sources from the 3C, 6C and 7C complete samples. Note the scarcity of sources with $P > 10^{27}\,\mathrm{W\,Hz^{-1}\,sr^{-1}}$ and with $D > 1\,\mathrm{Mpc}$.

The explanation for their absence comes from consideration of how the luminosity of a source with high jet-power evolves as it ages given the influence of the hotspot, together with the consequence of applying a flux-limit. This is illustrated in Fig. 5. Note that inclusion of the influence of the hotspot on the luminosity evolution of radio sources gives steeply declining tracks and hence obviates the need to invoke extremely steep density gradients in their environments, as suggested by [8, 9].

6 Young, distant radio galaxies

The combination of flux-limits and declining luminosity evolution point to an inevitable 'youth-redshift degeneracy' in any flux-limited sample. In a recent letter to *Nature* we examined the generality and ramifications of the youth-redshift degeneracy (Blundell & Rawlings 1999 [20]). We described how one especial advantage of the youth-redshift degeneracy is that very high-redshift sources, being inevitably very young, are seen after only a short time ($< 10^7$ yrs) after their jet-triggering event. A conclusion of that work was that detection of high-redshift ($z > 4$) sources thus enables a high-time-resolution study of triggering (and hence galaxy-merging) rates within a Gyr of the Big Bang.

Given their unique importance as cosmological probes (compared with say, the undateable optically selected high-z quasars), how then may we best find radio galaxies at extreme redshifts?

7 Searches for distant radio galaxies

In this conference we heard the exciting news of the discovery of the first $z > 5$ radio galaxy (Röttgering, these proceedings and van Breugel et al. 1999 [13]). The fundamental finding-frequency for the 'filtered' sample from which this object was found was 365 MHz which of course samples

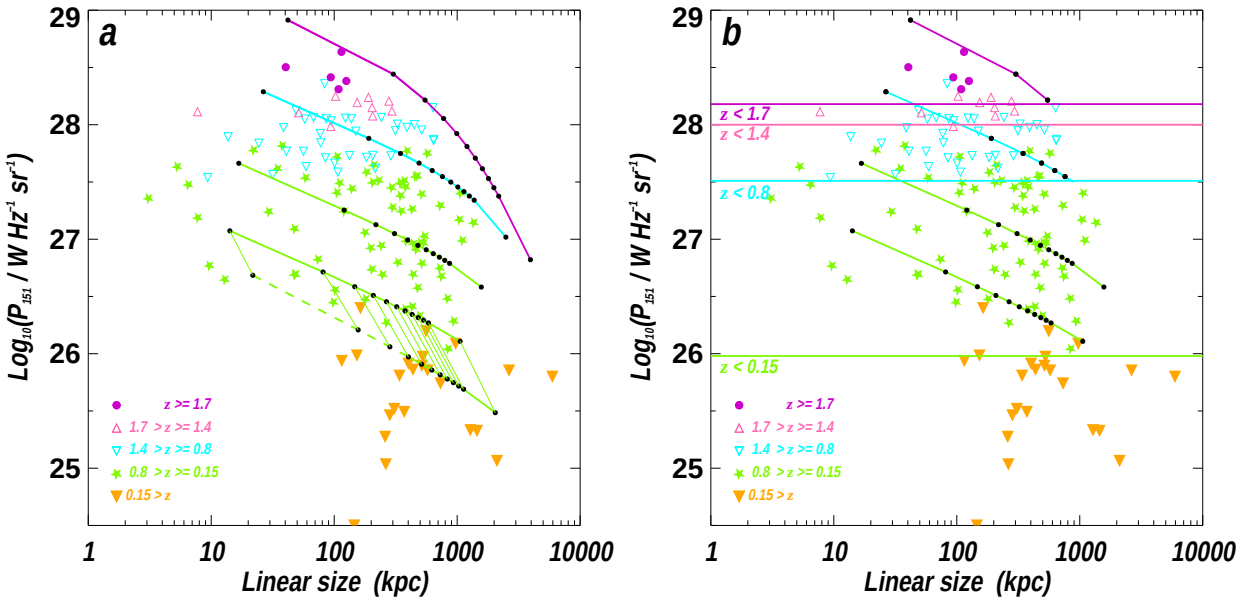

Figure 5: Overlaid on the 'P–D' plane for the 3C sample in **a** are model tracks tracing out the evolution of four example radio sources in luminosity and linear size, with from top to bottom $Q = 5 \times 10^{39}$ W at $z = 2$, $Q = 1 \times 10^{39}$ W at $z = 0.8$, $Q = 2 \times 10^{38}$ W at $z = 0.5$ and $Q = 5 \times 10^{37}$ W at $z = 0.15$. The dashed line indicates how the lower track luminosity reduces by $<$ half an order of magnitude if the ambient density becomes an order of magnitude lower. In **b** the horizontal lines represent the luminosities at which the flux-limit of 12 Jy takes its effect at the different redshifts indicated. A combination of the dramatically declining luminosity-with-age of the high-Q sources, their scarcity in the local Universe, together with the harsh reality of the flux-limit means that very powerful sources with large linear sizes are rarely seen.

emission at 2 GHz in the rest-frame of this object. Further filtering to favour the detection of high-redshift objects was performed by imposing a spectral index constraint on their sample of $\alpha > 1.3$ between 365 MHz and 1.4 GHz, and then further filtering using the infra-red K-band relation with redshift ([12, 11, 2]). However, an object at $z = 5$ will not be found by such a survey unless its GHz emission is sufficiently luminous. This requires that the source is sufficiently young that inverse Compton and synchrotron losses have not yet catastrophically depleted the emission in this GHz regime.

A significant advantage in searching for high-z radio galaxies is achieved using a *lower* fundamental finding-frequency. This is because of the steep spectrum of these objects and the avoidance of the frequency regime where inverse Compton and synchrotron losses are most manifest. Our own filtered samples, 6C★ [14] (from which Rawlings et al. found a $z = 4.4$ radio galaxy four years ago [15]) and the on-going 6C★★, have as their fundamental funding frequency 151 MHz, the frequency at which the 6C survey was undertaken by Hales et al. [16]. For radio galaxies at $z = 5$ it is their emission sampled at rest-frame 900 MHz which determines whether they exceed the flux-limit or not, and hence whether they will be members of the survey.

Searches for high redshift radio galaxies invariably make use of a spectral index constraint, since a steep spectral index is a characteristic of known high-redshift radio galaxies. This arises partly because of the 'k-correction' effect, partly because the more distant radio sources are more luminous so the P–α correlation takes effect and partly because of the z–$\alpha_{\rm GHz}$ correlation which comes from increased inverse Compton losses at high-redshift.

Fig. 6 shows schematically the contribution of the lobes, hotspots and core to the different frequency regimes in the radio wave-band. It also illustrates the different parts of the rest-frame spectrum probed by four recent/on-going searches for high-redshift galaxies. The first is the MG survey of Stern et al (1999), with the highest fundamental finding-frequency reviewed here of 5 GHz. (Their spectral index selection is made by cross-matching with a lower frequency of 1.4 GHz.) For $z = 5$ radio galaxies, their flux-limit at 5 GHz probes emission at 30 GHz in the rest-frame, where lobe emission is highly

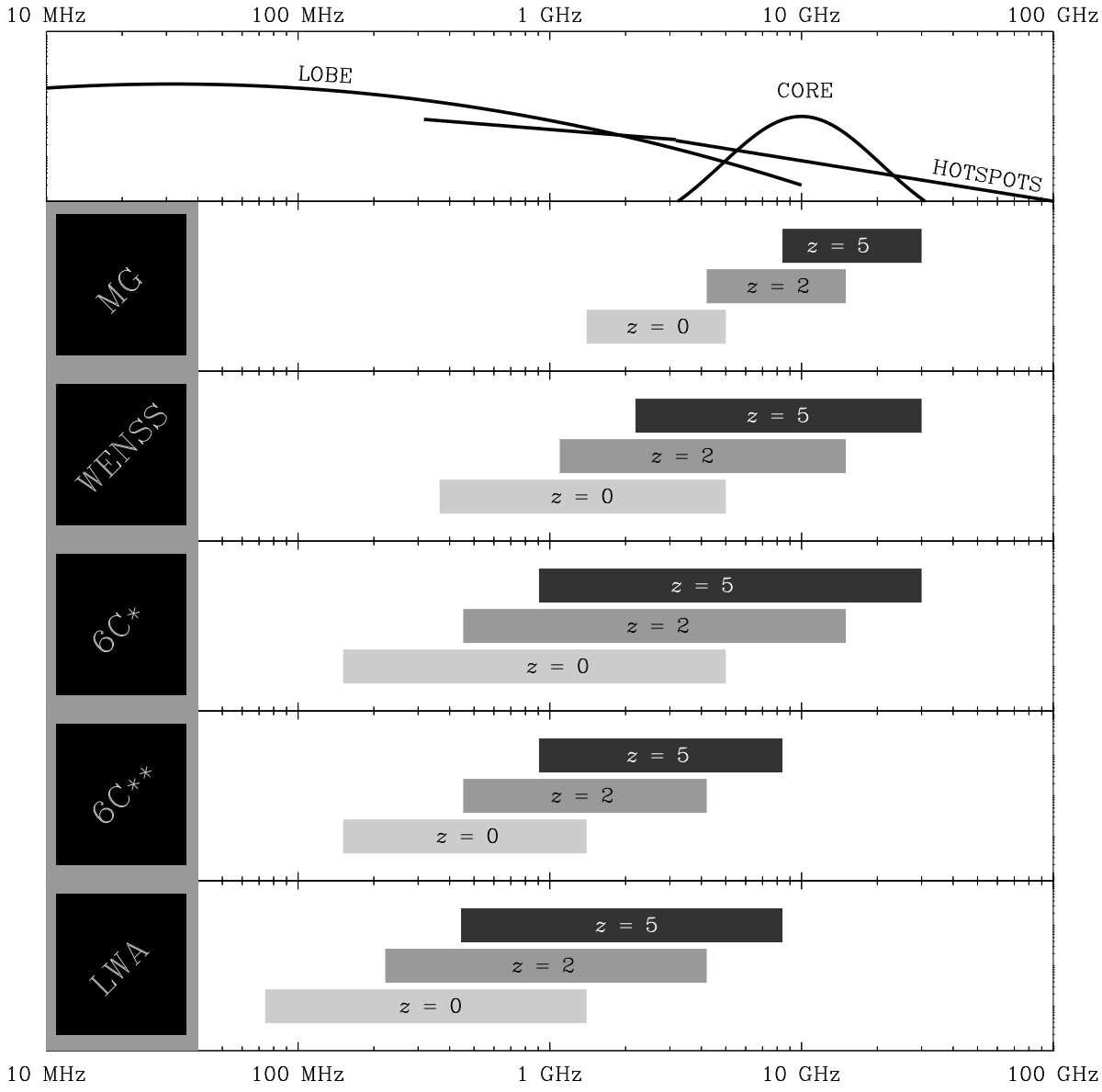

Figure 6: This figure indicates the different parts of the rest-frame spectrum which are probed for objects at $z = 0$, $z = 2$ and $z = 5$, by different strategies for finding high-z radio galaxies. See text for more details.

depleted. It is perhaps unsurprising then that this sample, although it contains one previously known $z = 3.6$ radio galaxy, did not find any other $z > 3$ objects.

Surveys with a lower fundamental finding-frequency are much less vulnerable to incompleteness: the WENSS survey of van Breugel, Röttgering and collaborators which has found the first $z > 5$ radio galaxy, has its finding-frequency still in the GHz rest-frame regime together with other filtering criteria depending on the K–z relation. These make completeness somewhat tricky to model.

Both the 6C★ and 6C★★ samples have as their fundamental finding-frequency 151 MHz in the observed frame. Our selection criteria were chosen to minimize excessive contamination from low-redshift interlopers *without excluding members of the target population.* These precautions are necessary for meaningful statements to be made about the veracity of the purported 'redshift-cutoff' in the co-moving space density of radio galaxies (Jarvis et al. *in prep*).

The lowest plot indicates a survey which should be possible with the currently evolving low frequency array concepts at NRL and NFRA, LWA and LOFAR respectively. This plot indicates that part of the spectrum which would be sampled by a finding-frequency of 75 MHz (450 MHz in the rest-frame of a

$z = 5$ radio galaxy).

A disadvantage of the 151-MHz 6C survey however, is its relatively low spatial resolution (4 arcmin). The problem of confusion is a significantly greater one in the deeper 6C★★ sample than in the 6C★ sample. This then clearly identifies the two-pronged strategy which it is hoped will shape the future capabilities of LWA/LOFAR. The unprecedented combination of *low frequency and high-resolution is the key to the high-redshift Universe.*

The youth-redshift degeneracy, mentioned in §6, means that there is a wide and increasingly ill-defined gulf between the luminosity function (the co-moving space density of the super-set of the radio-sources which make it above the various survey flux-limits) and the birth function of radio sources. We have performed many Monte-Carlo runs of simulated complete and filtered samples to constrain the birth function of radio sources. Comparison of these with our own observed complete and filtered samples is the only means to constrain the birth-function of radio sources throughout cosmic history (Blundell, Rawlings & Willott, in prep.). LWA/LOFAR should enable this to be constrained at the very earliest epochs that classical double radio sources are triggered.

References

[1] Laing, R. A., Riley, J. M. & Longair, M. S. *MNRAS*, **204**, 151–187 (1983).

[2] Rawlings, S., Blundell, K.M., Lacy, M., Willott, C.J. & Eales, S.A., in *'Observational Cosmology with the new radio surveys'*, eds M.N. Bremer, N. Jackson and I. Pérez-Fournon, Kluwer Academic Publishers, p171, (1998).

[3] Kapahi, V. K., Subrahmanya, C. R. & Kulkarni, V. K. *J. Astrophys Astron.*, **8**, 33–50 (1987).

[4] Neeser, M.J., Eales, S.A., Law-Green, J.D., Leahy, J.P., & Rawlings, S., *ApJ*, **451**, 76–87, (1995).

[5] Blundell, K. M., Rawlings, S. & Willott, C. J. *AJ*, **117**, 677–706 (1999).

[6] McCarthy, P., in 'The most distant radio galaxies', KNAW colloquium, Amsterdam eds Best et al, (1997).

[7] Scheuer, P.A.G., *MNRAS*, **166**, 513–528 (1974).

[8] Baldwin, J. E. in *Extragalactic radio sources* (eds Heeschen, D. S. & Wade, C. M.) 21–24 (Proc. of the 97 IAU Symp. Reidel, Dordrecht, 1982).

[9] Kaiser, C. R., Dennett-Thorpe, J. & Alexander, P. *Mon. Not. Roy. Astr. Soc.* **292**, 723–732 (1997).

[10] Lacy, M., Rawlings, S., Hill, G.J., Bunker, A.J., Ridgway, S. & Stern, D., *MNRAS*, astro-ph/99905358 (1999).

[11] Eales, S.A. & Rawlings, S., *ApJ*, **460**, 68–93, (1996).

[12] Lilly, S.J. & Longair, M.S., *MNRAS*, **211**, 833–855

[13] van Breugel, W., de Breuck, C., Stanford, S.A., Stern, D., Röttgering, H., Spinrad, H., Miley, G., *ApJ*, **518**, L61–L64 (1999).

[14] Blundell, K.M., Rawlings, S., Eales, S.A., Taylor, G.B., & Bradley, A.D., *MNRAS*, **295**, 265–279 (1998).

[15] Rawlings, S., Lacy, M., Blundell, K. M., Eales, S. A., Bunker, A. J. & Garrington, S. T. *Nature* **383**, 502–505 (1996).

[16] Hales, S.E.G., Baldwin, J.E., & Warner, P.J., *MNRAS*, **234**, 919–936 (1988).

[17] Leahy, J.P., Black, A.R.S., Dennett-Thorpe, J., Hardcastle, M.J., Komissarov, S., Perley, R.A., Riley, J.M., & Scheuer, P.A.G., *MNRAS*, **291**, 20–53 (1997).

[18] Black, A.R.S., Baum, S.A., Leahy, J.P., Perley, R.A., Riley, J.M., Scheuer, P.A.G., *MNRAS*, **256**, 186–208 (1992).

[19] Hardcastle, M.J., Alexander, P., Pooley, G.G., Riley, J.M., *MNRAS*, **288**, 859–890 (1997).

[20] Blundell, K. M. & Rawlings, S. *Nature* **339**, 330–332 (1999).

[21] Stern, D., Dey, A., Spinrad, H., Maxfield, L., Dickinson, M., Schlegel, D. & González, R.A. *AJ*, **117**, 1122–1138 (1999).

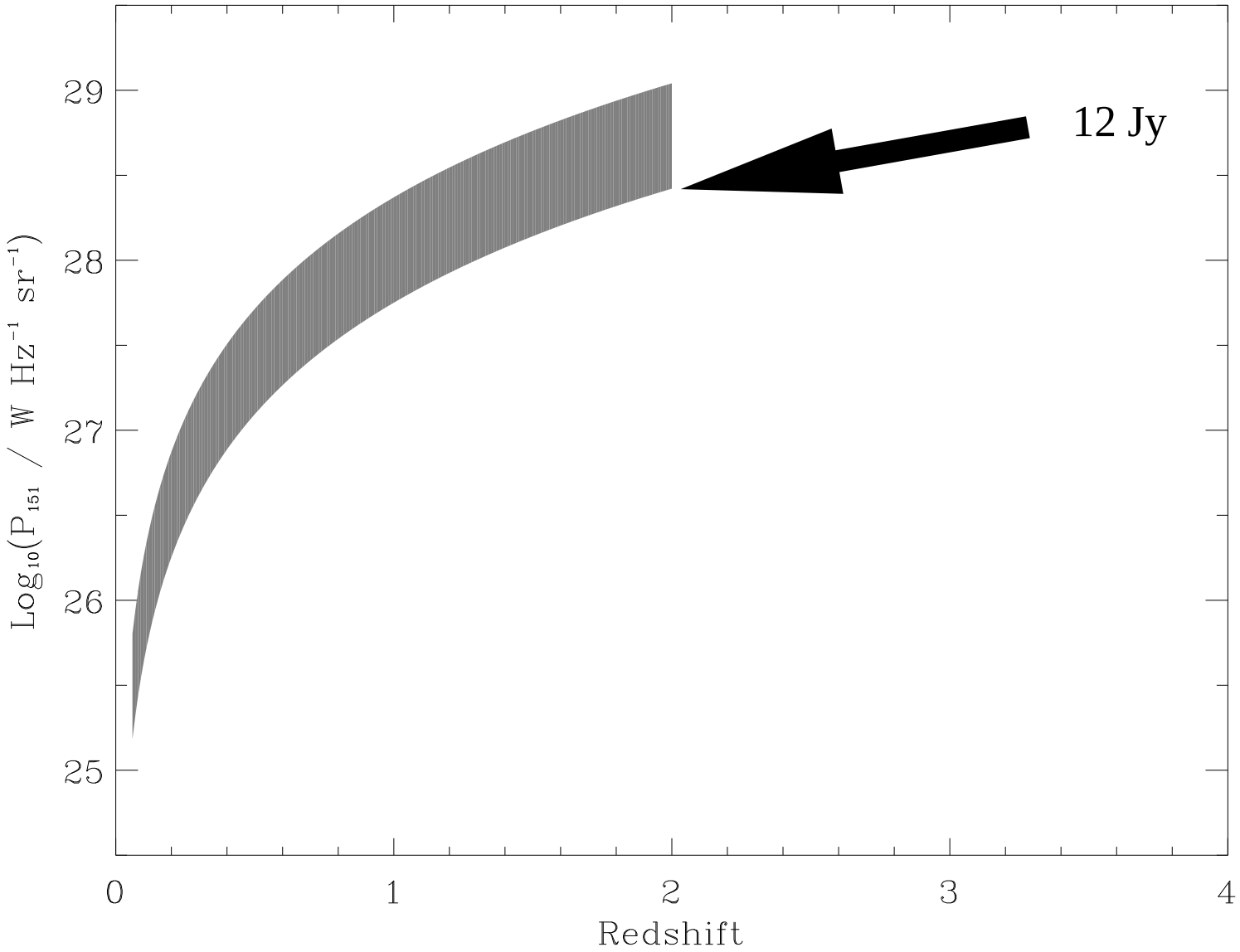
12 Jy
29
28
27
26
25
0
1
2
3
4
Redshift
Log10(P151 / W Hz-1 sr-1)

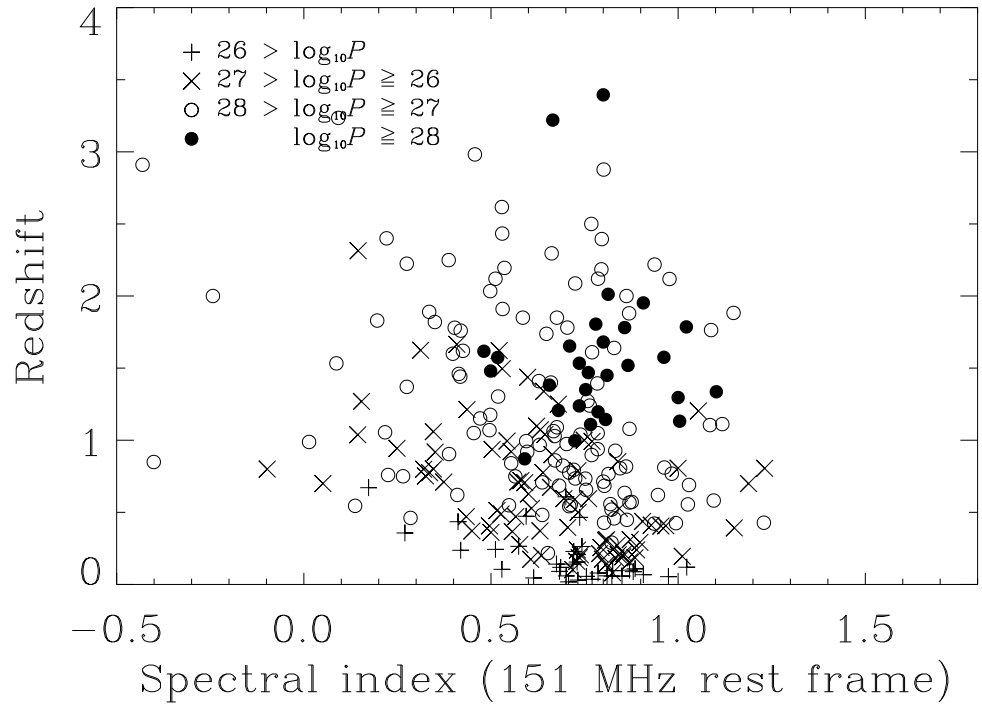
+ 26 > log10P
× 27 > log10P ≧ 26
○ 28 > log10P ≧ 27
● log10P ≧ 28
Redshift
0
1
2
3
4
−0.5
0.0
0.5
1.0
1.5
Spectral index (151 MHz rest frame)

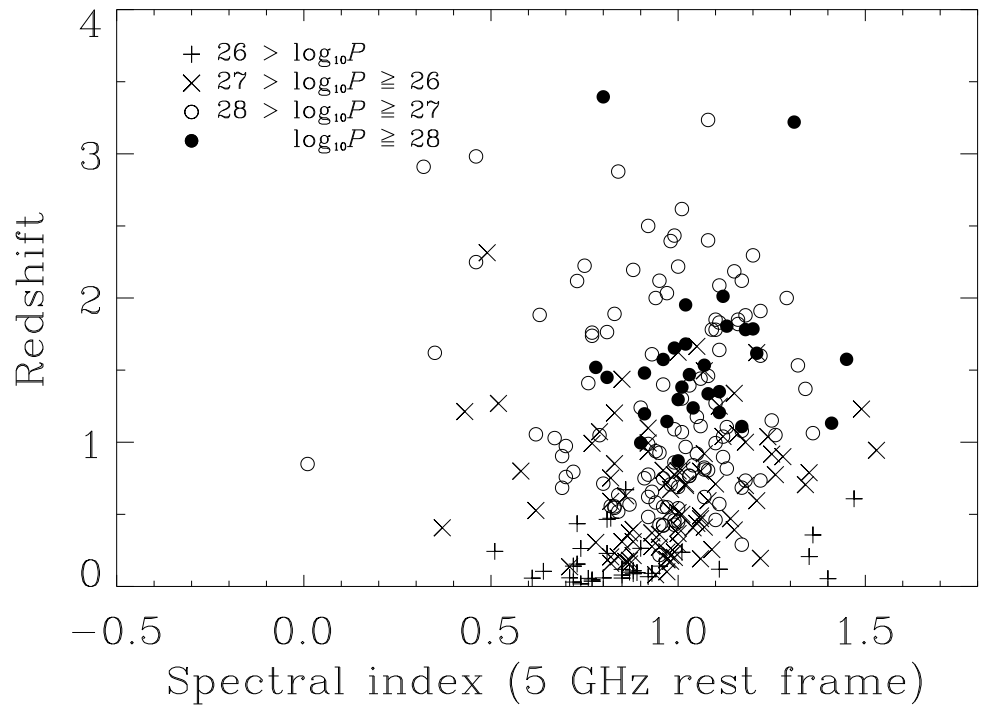
+ 26 > log10P
× 27 > log10P ≧ 26
○ 28 > log10P ≧ 27
● log10P ≧ 28
Redshift
0
1
2
3
4
−0.5
0.0
0.5
1.0
1.5
Spectral index (5 GHz rest frame)

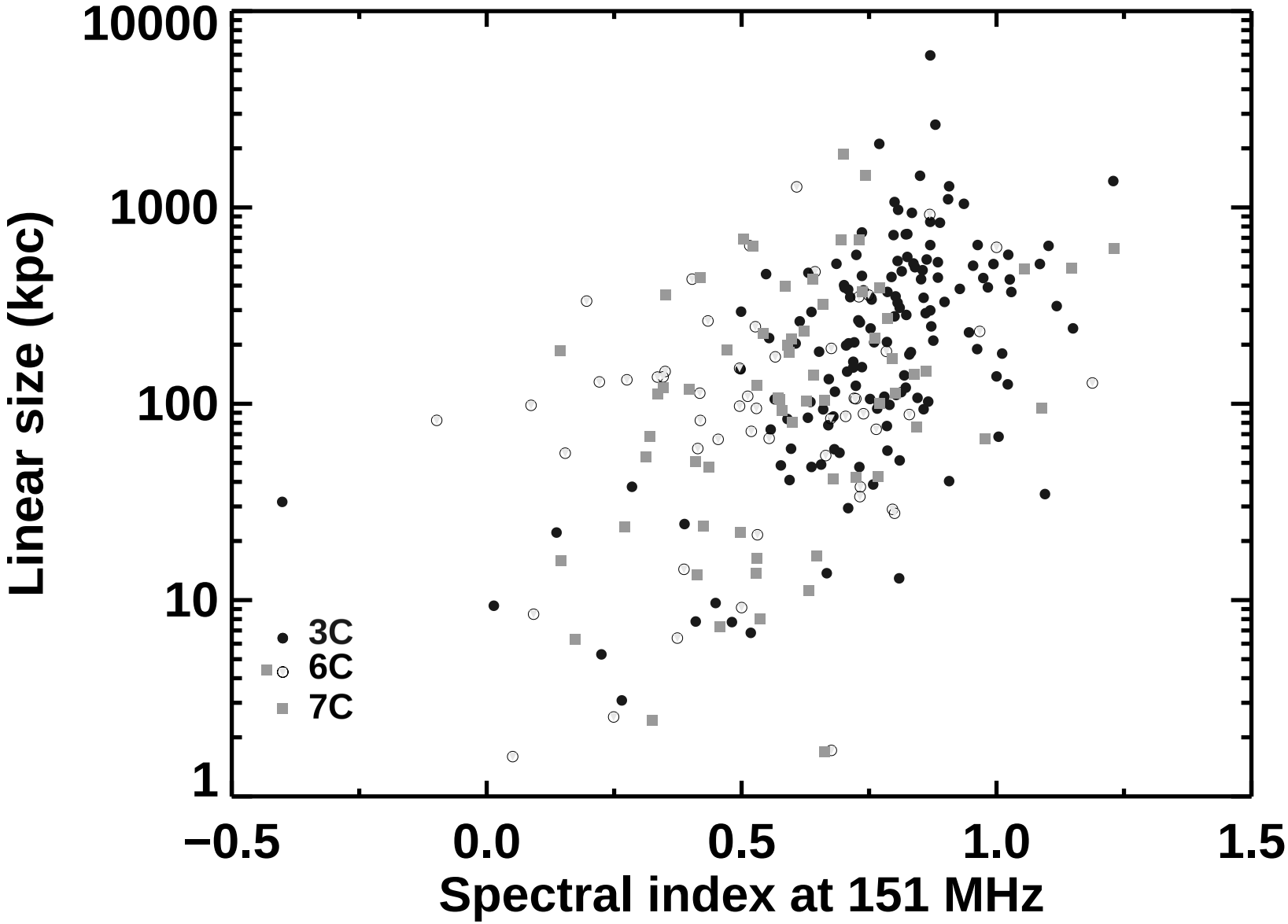
10000
1000
100
10
1
Linear size (kpc)
3C
6C
7C
−0.5
0.0
0.5
1.0
1.5
Spectral index at 151 MHz

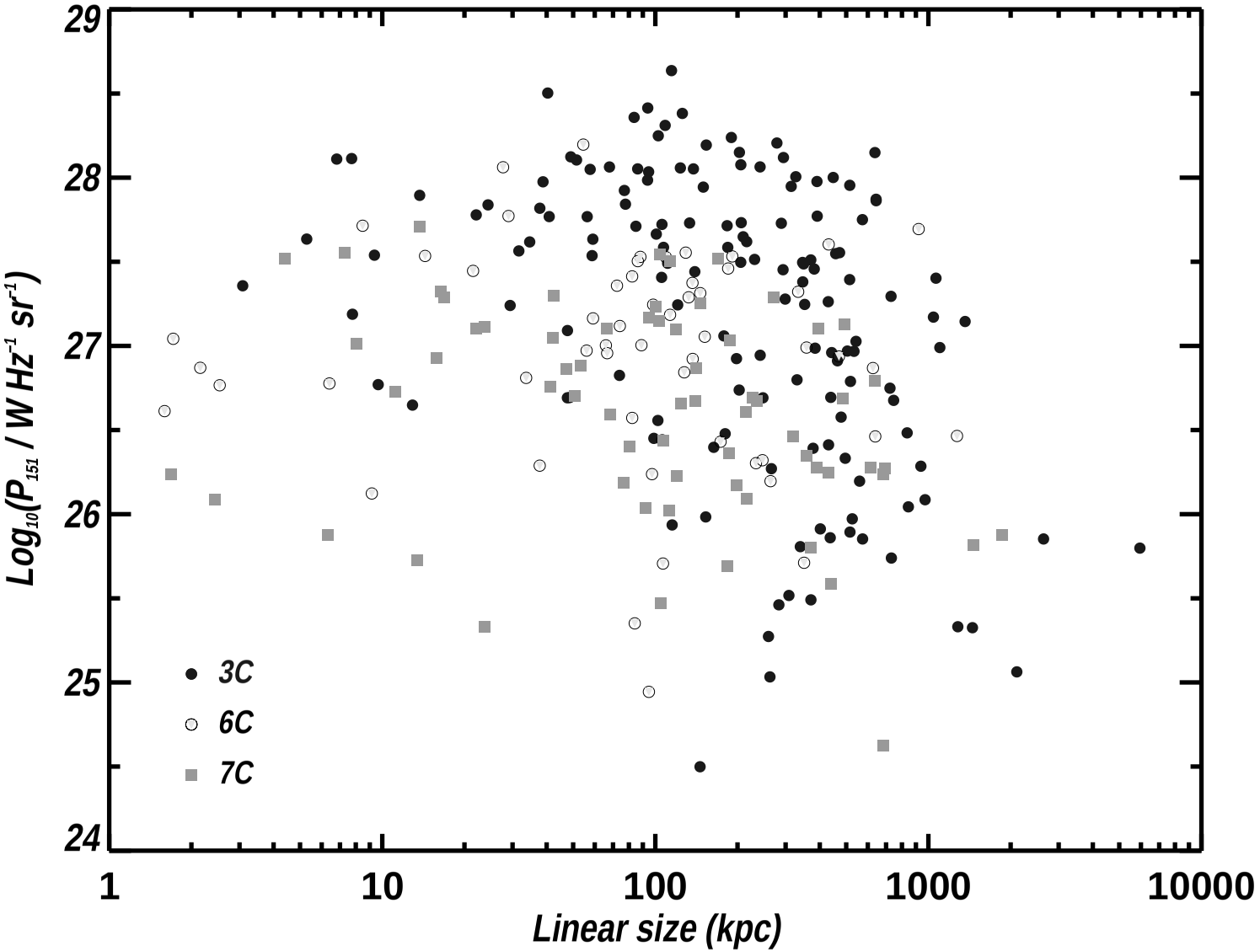
29
28
27
26
25
24
1
10
100
1000
10000
Log10(P151 / W Hz-1 sr-1)
Linear size (kpc)
3C
6C
7C

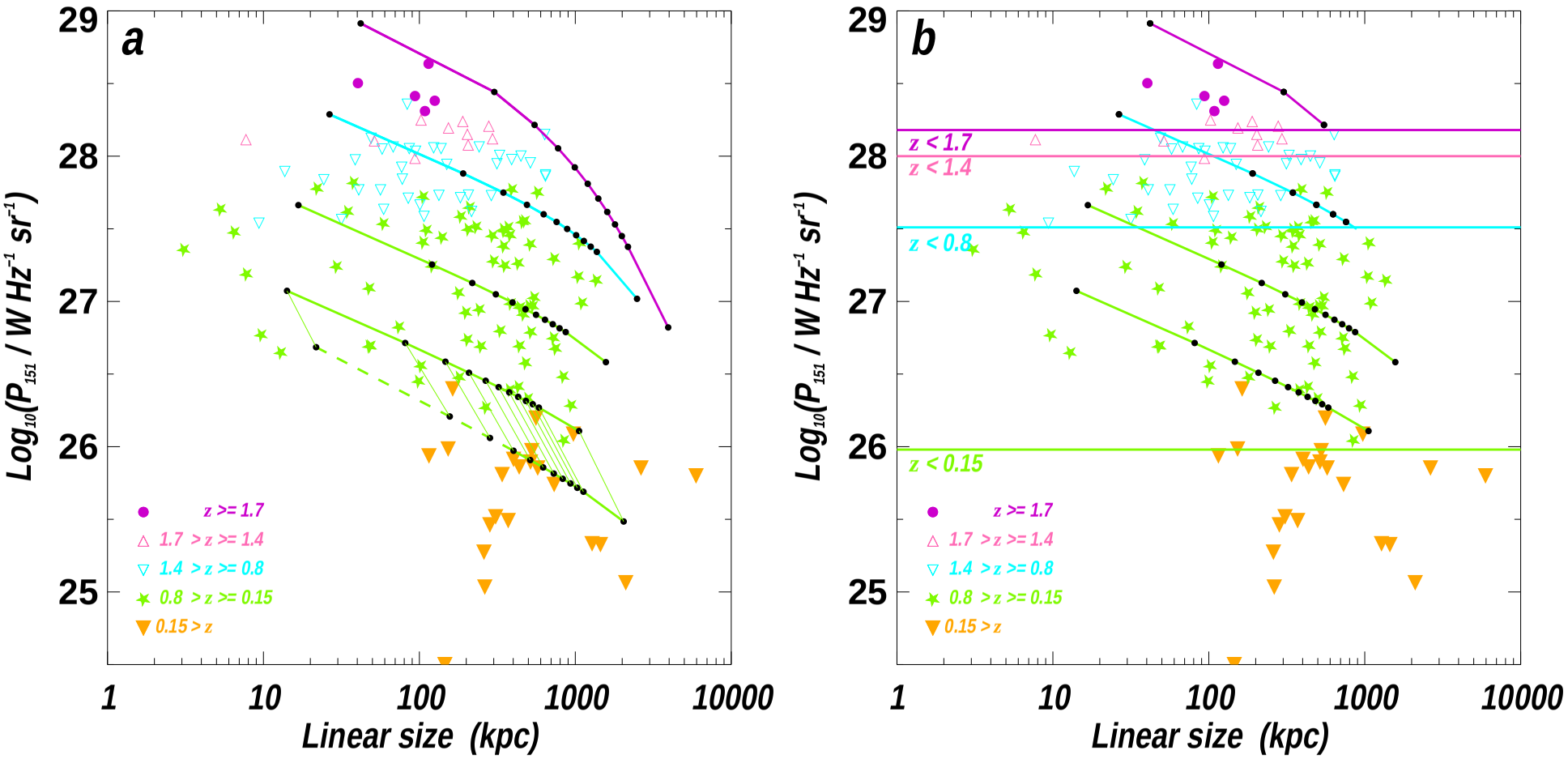
a
b
29
28
27
26
25
1
10
100
1000
10000
Linear size (kpc)
Log10(P151 / W Hz-1 sr-1)
z >= 1.7
1.7 > z >= 1.4
1.4 > z >= 0.8
0.8 > z >= 0.15
0.15 > z
z < 1.7
z < 1.4
z < 0.8
z < 0.15

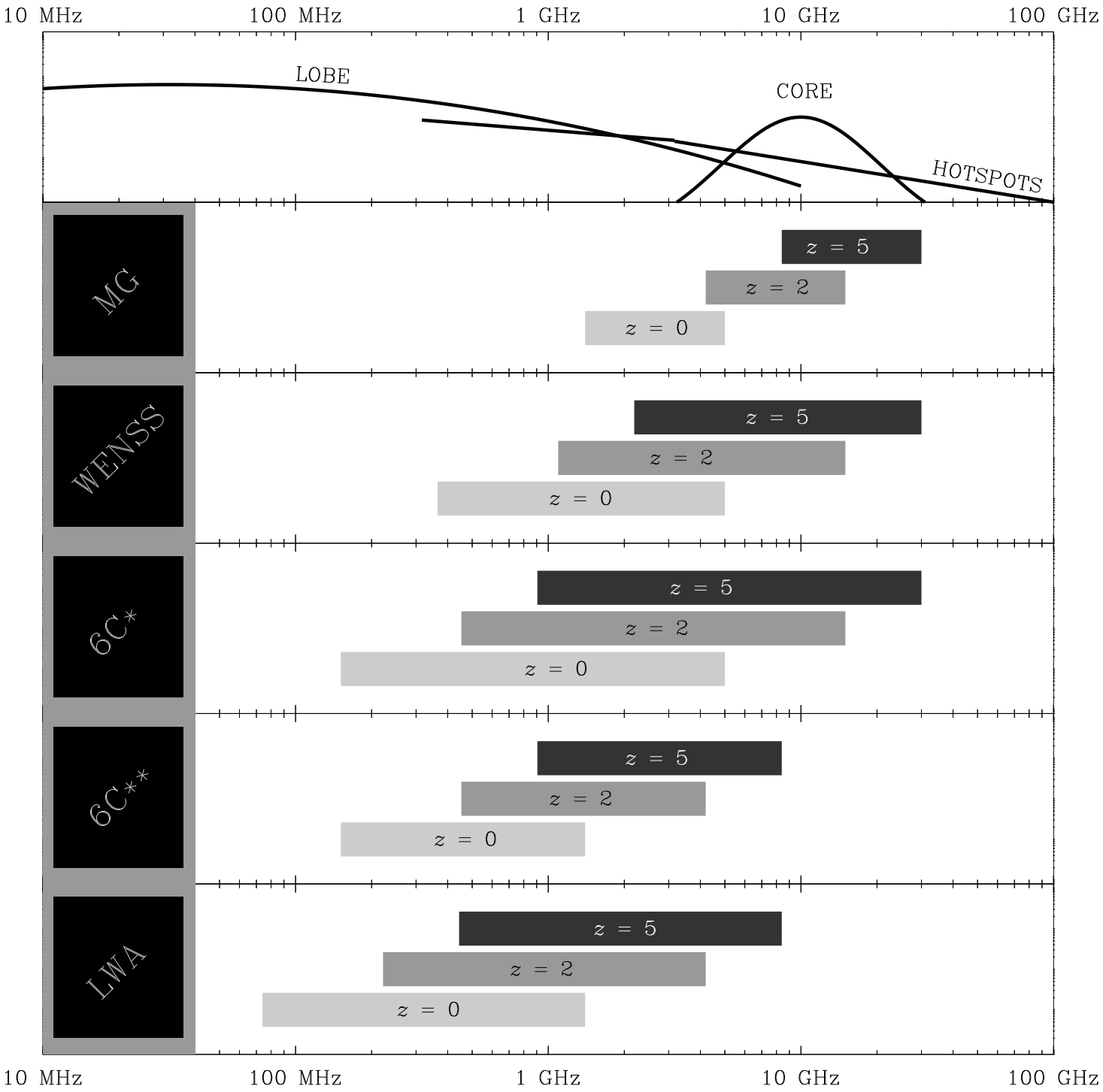
10 MHz
100 MHz
1 GHz
10 GHz
100 GHz
LOBE
CORE
HOTSPOTS
MG
WENSS
6C*
6C**
LWA
z = 5
z = 2
z = 0